RESEARCH ARTICLE

Monitoring microRNAs Using a Molecular Beacon in CD133+/ CD338+ Human Lung Adenocarcinoma-initiating A549 Cells

Quan Yao[1], Jian-Guo Sun[2], Hu Ma[3], An-Mei Zhang[2], Sheng Lin[4], Cong-Hui Zhu[2], Tao Zhang[1]*, Zheng-Tang Chen[2]*

Abstract

Lung cancer is the most common causes of cancer-related deaths worldwide, and a lack of effective methods for early diagnosis has greatly impacted the prognosis and survival rates of the affected patients. Tumor-initiating cells (TICs) are considered to be largely responsible for tumor genesis, resistance to tumor therapy, metastasis, and recurrence. In addition to representing a good potential treatment target, TICs can provide clues for the early diagnosis of cancer. MicroRNA (miRNA) alterations are known to be involved in the initiation and progression of human cancer, and the detection of related miRNAs in TICs is an important strategy for lung cancer early diagnosis. As Hsa-miR-155 (miR-155) can be used as a diagnostic marker for non-small cell lung cancer (NSCLC), a smart molecular beacon of miR-155 was designed to image the expression of miR-155 in NSCLC cases. TICs expressing CD133 and CD338 were obtained from A549 cells by applying an immune magnetic bead isolation system, and miR-155 was detected using laser-scanning confocal microscopy. We found that intracellular miR-155 could be successfully detected using smart miR-155 molecular beacons. Expression was higher in TICs than in A549 cells, indicating that miR-155 may play an important role in regulating bio-behavior of TICs. As a non-invasive approach, molecular beacons could be implemented with molecular imaging to diagnose lung cancer at early stages.

Keywords: microRNA - non-small cell lung cancer - tumor-initiating cell - molecular beacon - molecular imaging

Asian Pac J Cancer Prev, **15 (1)**, 161-166

Introduction

Lung cancer is the leading cause of cancer-related mortality worldwide, and its total 5-year survival rate is approximately 15 % for non-small cell lung cancer (NSCLC) (Jemal et al., 2006). The current screening strategies based on chest radiography are inefficient for detecting lung cancer in its early stage (Henschke et al., 2006), and a lack of effective methods for early diagnosis has greatly impacted the prognosis and survival rate of this cancer. Thus, it is important to develop new diagnostic methods of early diagnosis.

Tumor-initiating cells (TICs) possess a strong self-renewal capacity and multiplex differentiation potential and are considered to be the main responsible for tumorigenesis, resistance to tumor therapy, metastasis, and recurrence (Guo et al., 2006; Adhikari et al., 2011). As TICs are thought to be the major basis for therapeutic intervention and a potential therapeutic target, TICs can provide new clues for the early diagnosis of cancer.

Lung cancer TICs were first isolated by Eramo et al., who found CD133-positive tumorigenic cells in both SCLC and NSCLC tissues. CD133-positive lung CSCs (LCSCs) display a high expression level of ABCG2 (CD338), an ATP-binding cassette (ABC) transporter, which is thought to be responsible for resistance to such chemotherapeutic agents as cisplatin (Zhou et al., 2001; Bertolini et al., 2009). TICs are also present in established lung cancer cell lines, including H460 and A549, which show tumor-initiating capacity in mice and chemotherapeutic drug resistant due to the elevated expression of ABCG2 (Ho et al., 2007).

MicroRNAs (miRNAs) are small non-coding single-stranded RNA molecules (19 to 25 nt) that regulate gene expression at a post-transcriptional level (Bartel, 2004; Bushati and Cohen, 2007; Krol et al., 2010). miRNAs can regulate cancer cell differentiation, proliferation, survival, and metastasis, acting as oncogenes or tumor suppressors by regulating the expression of downstream genes through different cancer development and progression

*[1]Diagnosis and Treatment Center of Cancer, Chengdu Military General Hospital, Chengdu, [2]Institute of Cancer, Xinqiao Hospital, Third Military Medical University, Chongqing, [3]Department of Oncology, Affiliated Hospital of Zunyi Medical University, Zunyi, [4]Department of Oncology, Affiliated Hospital of Luzhou Medical College, Luzhou, China *For Correspondence: zhtao269@yeah.net, chenzhtang@yeah.net*

pathways (Chen, 2005; Garzon et al., 2009; Kwak et al., 2010; Zandberga et al., 2013). Accordingly, these molecules could constitute a powerful therapeutic strategy for interfering with cancer initiation and progression (Garofalo and Croce, 2011). Moreover, miRNAs have been implicated in the control of self-renewal in stem cells (Hatfield and Ruohola-Baker, 2008). Georgantas et al. found that miRNA-155 played a role in normal human myelopoiesis, lung differentiation, and erythropoieis, and a recent study has shown that a high level of hsa-miR-155 is associated with a poor outcome in lung cancer (Georgantas et al., 2007; Wang et al., 2009b). Thus, the detection of related miRNAs in TICs is an important strategy for the early diagnosis of lung cancer. A molecular beacon (MB) is a highly sensitive detection tool that can be used in the study of miRNA visualization in living cells and may provide technical support for tumor diagnosis.

In this study, TICs were isolated from A549 cells by applying an immune magnetic bead isolation system. miR-155 MBs were then used to detect miR-155 gene expression in TICs. As a non-invasive imaging method, MBs could be used to detect miRNAs in lung cancer.

Materials and Methods

Isolation and culture of TICs from the A549 cell line

The A549 cell line was obtained from ATCC (American Type Culture Collection, Manassas, VA.). This human NSCLC cell line was cultured in RPMI-1640 (Hyclone) medium supplemented 10% heat-inactivated fetal bovine serum (FBS; PAA), penicillin (100 U/mL; Hyclone), and streptomycin (100 μg/mL; Hyclone). According to the manufacturer's instructions, approximately 108/ 300 μl of cells were incubated with 10 μl CD133/1 from Miltenyi Biotec (Bergisch Gladbach) microbeads for 15 min and 20 μl CD338/1 from Miltenyi Biotec (Bergisch Gladbach, Germany) for 10 min. The cells were then sorted using a magnetic activated cell sorting (MACS) separator from Miltenyi Biotec (Bergisch Gladbach). The sorted cells were grown in serum-free DMEM/F12 (Hyclone) medium containing 0.4% BSA, 50 μg/ml insulin (Sigma), 20 μg/ml basic fibroblast growth factor (bFGF, Sigma), and 20 μg/ml human recombinant epidermal growth factor (EGF, Sigma). All cells were incubated at 37 °C in a humidified atmosphere containing 5% CO_2.

Flow cytometry analysis

Spheres were dissociated into single cells, washed, and incubated with monoclonal antibodies specific for human APC-conjugated CD133/1and PE-conjugated ABCG2 (CD338, Miltenyi Biotec). The appropriate dilution and procedures were performed according to the manufacturer's instructions. After incubation for 30 min, the cells were washed again and analyzed using flow cytometry.

Immunofluorescence

Spheroids were centrifuged onto slides using a cytospin, fixed with 4% paraformaldehyde for 20 min, and blocked with normal serum for 30 min at room temperature. The slides were then incubated with rabbit monoclonal anti-CD133 (Abcam) and goat polyclonal anti-ABCG2 antibodies (Santa Cruz) at dilution of 1:300 and stored overnight at 4°C protected from light. After washing, the slides were incubated with FITC-conjugated goat anti-rabbit IgG (Beyotime Biotec, China) and Cy3-conjugated donkey anti-goat IgG (Biolegend) fluorescent antibodies at a dilution of 1:400 for 30 min. After DAPI staining for nuclei, the slides were examined by confocal microscopy.

Cell proliferation assays

The A549 cells and TICs were plated in a 96-well plate (2000 cells/well) and supplemented with the corresponding growth medium. At the end of the treatments, 10μl of the WST-1 Cell proliferation Assay Kit (Beyotime Biotec, China) was added to each well, and the cells were incubated in a cell culture incubator for 2 hours. The plate was shaken for 1 minute on a shaker, and the absorbance was measured using a microplate reader at 450 nm; the reference wavelength was set to more than 600 nm.The absorbance of each well was measured for five days.

Quantitative Real-time RT-PCR

The isolation of total RNA was performed using RNAiso Plus (Takara) according to the manufacturer's instructions. The mRNA levels were analyzed by quantitative real-time RT-PCR using an ABI 7500 real-time PCR System. The following human miR-155 reverse transcription-specific primer was synthesized: 5'-GTCGTATCCAGTGCAGGGTCCGAGGTATTCGC ACTGGATACGACACCCCT-3'The U6 reverse transcription primer was synthesized according to the PCR reverse primer. Reverse transcription was performed with the PrimeScript RT reagent kit (Takara) at 42 °C for 15 min and 85 °C for 5 s. The primer sequences used in the real-time RT-PCR were asfollows: 5'-GAACTCCCT GAAAAGAGATGCAC-3' (sense primer for human CD133) and 5'-CCTGTGCGTTGAAGTATCTTGAC-3' (antisense primer for human CD133); 5'-CGAAAGAGA AAGCGAACCAGTATC-3' (sense primer for human OCT-4) and 5'-TACAGAACCACACTCGGACCAC-3' (antisense primer for human OCT-4); 5'-GAGCAGGAG GAGTTGGGTTCT-3' (sense primer for human Nestin) and 5'-GAGTGGAGTCTGGAAGGGTCTC-3' (antisense primer for human Nestin); 5'-CACAAAAGTCTGGAA GGGTCTC-3' (sense primer for human CD338 gene) and 5'-GCACACAGAAACACAACACTTGG-3' (antisense primer for human CD338); 5'-GACAGTAAATGGGG AACAACTGG-3' (sense primer for human CD326) and 5'-GCAACAACTGCTATCACCACAAC-3' (antisense primer for human CD326); 5'-CGGCGGTTAATGCTAA TCGTG-3' (sense primer for human miR-155) and 5'-GTGCAGGGTCCGAGGT-3' (antisense primer for human miR-155); 5'-CTCGCTTCGGCAGCACA-3' (sense primer for human U6) and 5'-AACGCTTCACGAATTTGCGT-3' (antisense primer for human U6); 5'-GTGAAGGTGACAGCAGTCGGTT -3' (sense primer for human β-actin) and 5'-GAAGTGGGGTGGCTTTTAGGA -3' (antisense primer for human β-actin). The reactions for the CD133,

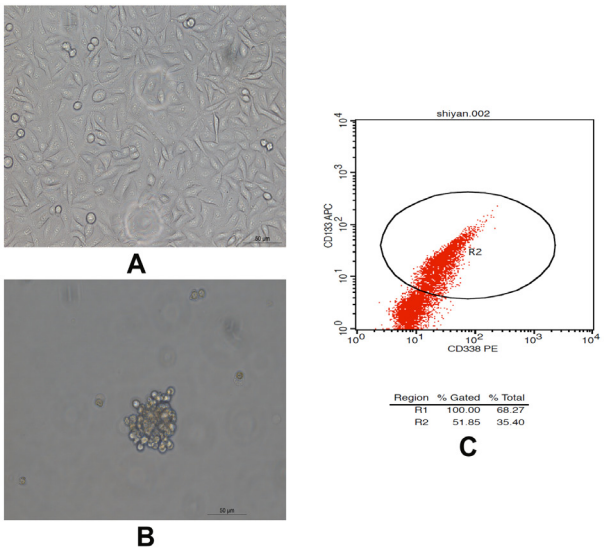

Figure 1. Separation of the CD133⁺/CD338⁺ Subpopulation from A549 Cells by MACS. (A) Cytometric CD133/CD338 expression in normal A549 cells; (B) secondary passage CD133⁺/CD338⁺ spheroids, (C) The flow cytometry analysis of CD133⁺/CD338⁺ cells (200×)

Nestin, OCT-4, CD338, CD326, and β-actin genes were performed under the following conditions: one cycle at 95°C for 30 s and 40 cycles at 95°C for 3 s and 58°C for 34 s. The PCR conditions for the hsa-miR-155 and U6 genes were: one cycle at 95 °C for 30 s, followed by 40 cycles of 95 °C for 15 s and 58 °C for 30 s. The fold changes in the levels of CD133, Nestin, OCT-4, CD338, and CD326 were calculated relative to β-actin. The fold changes in the levels of miR-155 levels were calculated relative to the endogenous U6 control. Each reaction was performed in triplicate.

Generation of subcutaneous lung cancer xenografts

All animal experiments were conducted with the approval of the Institutional Animal Care and Use Committee of the Xinqiao Hospital and Chengdu General Military General Hospital Institute for Biological Sciences. Four-week-old male nude mice were purchased from the Chinese Academy of Medical Sciences (Beijing, China). To generate xenografts, CD133⁺/CD338⁺ cells and A549 cells were injected subcutaneously on the right side respectively. 1×10^3, 1×10^4, and 1×10^5 CD133⁺/CD338⁺ cells in 100 μl suspensions were injected; 1×10^4, 1×10^5, and 1×10^6 A549 cells were injected. The mice were observed twice a week and sacrificed at six weeks.

MBs synthesis, Hoechst 33342 staining and laser-scanning confocal microscopy

Random sequence MBs (Negative control MBs) and hsa-miR-155-specific MBs were designed as follows: Random sequence MB, 5'-Alexa488-CCAGCG-ac+Gcca+Atg+Acc+Tta+Agcattaa-CGCTGG-BHQ1-3'; Hsa- miRNA-155 MB, 5'-Alexa488-CCAGCG-acccc+Ta+Tcac+Gat+Tagc+Attaa-CGCTGG-BHQ1-3', The underlined bases are the bases added to form a stem with an optimal Tm, and the +N represents the LNA base. The two MBs labeled with Alexa488 were synthesized by Takara, Japan. All of the transient transfections

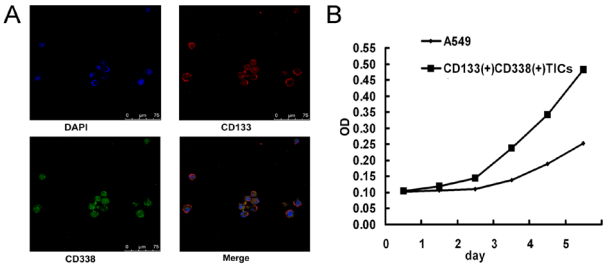

Figure 2. Immunofluorescence and Cell Proliferation Assays of the CD133⁺/CD338⁺ Subpopulation of A549 as TICs. (A) Immunofluorescence of CD133 (red) and CD338 (green) expression on spheroids. (B) Cell proliferation assays of the CD133⁺/CD338⁺ subpopulation

were performed in triplicate. A hybridization study was performed according to previous research (Kim et al., 2007; Yao et al., 2012). CD133⁺/CD338⁺ cells were seeded in the wells of culture plates for confocal microscopy (1×10^3 cells/well). The cells were washed with phosphate-buffered saline (PBS; Boster, China) three times after MB delivery with the the siPORT NeoFX transfection agent (Ambion, USA). A 300 µl aliquot of Hoechst 33342 (Beyotime, China) was then added to each well. Images of the living cells containing MBs were obtained using a Leica TCS SP5 confocal microscope with an HCX PL APO CS 40x/1.25 PH3 oil-immersion objective. The mean fluorescence intensity was calculated using Software Image-Pro Plus Version 5.1 (Media-Cybernetics, Bethesda, MD).

Statistical analysis

The data are presented as the mean ± SD. A statistical analysis was performed using an independent-samples t-test, and differences were considered statistically significant at $p<0.05$.

Results

Isolation and identification of CD133⁺/CD338⁺ cells from the A549 cell line

Normal A549 cells grew as monolayer squamous cells, attaching to the culture flask (Figure 1A). CD133⁺/CD338⁺ cells were sorted grew into spheres in a serum-free medium (Figure 1B). The CD133⁺/CD338⁺ cells were identified using flow cytometry, and we found that the expression of CD133 and CD338 was approximately 35.4% on the CD133⁺/CD338⁺ cells (Figure 1C).

Immunofluorescence and cell proliferation assays

Immunofluorescence of the 5th sphere progeny showed that most of the spheroids were positive for CD133 and CD338 (Figure 2A). Cell proliferation assays demonstrated that a strong proliferation capacity of the CD133⁺/CD338⁺ cells are stronger than A549 cells (Figure 2B).

Quantitative real-time RT-PCR and in vivo subcutaneous xenografts

Stem cell-associated genes, including CD133, OCT-4, Nestin, CD326, and CD338, were more highly expressed,

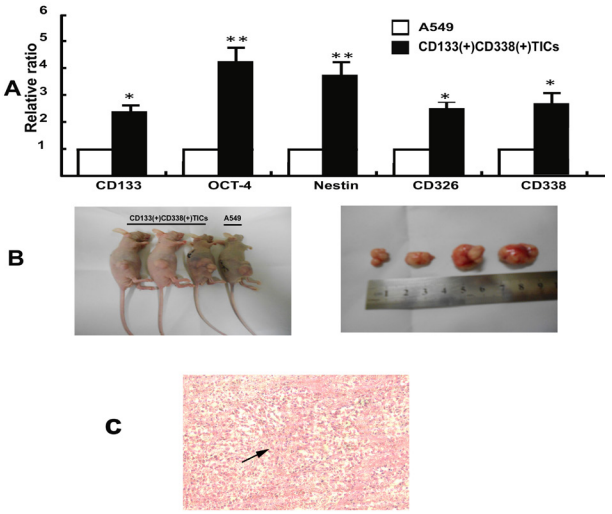

Figure 3. Quantitative Real-time RT-PCR and *in Vivo* Subcutaneous Xenografts. (A) Detection of stem cell-associated genes between the CD133+/CD338+ cells and normal A549 cells by quantitative RT-PCR (*p<0.05; **p<0.01); (B) Subcutaneous xenografts on nude mice (left panel:the left three mice were injected with 1×10^5 , 1×10^5 and 1×10^6 CD133+/CD338+ cells respectively; the right mouse were injected with 1×10^6 normal A549 cells.right panel:the responding subcutaneous xenografts were obtained from the left panel mice); (C) all mice were sacrificed at 6 weeks after injection and observed by histology (200×)

Table 1. Subcutaneous Xenografts on Nude Mice (male, 4-week-old)

Cell number	1×10^3	1×10^4	1×10^5	1×10^6
CD133+/CD338+ cells	0/3	3/3	3/3	
A549 cells		0/3	0/3	3/3

by more than two-fold, in the CD133+/CD338+ cells compared to the A549 cells (Figure 3A). Furthermore, in vivo subcutaneous xenografts on nude mice showed that only 1×10^4/ml CD133+/CD338+ cells could generate xenografts, whereas, 1×10^5/ml A549 cells failed to do so (Figure 3B and Table 1). These results demonstrate that CD133+ /CD338+ cells have a stronger capability of tumorigenesis than A549 cells. As shown by H&E staining (Figure 3C), xenograft tumor tissue displayed characteristic glandular structures. This indicates that xenograft tumor was adenocarcinomas.

miR-155 gene expression in CD133+/CD338+ cells

The results of the MB specificity for the detection of miRNA-155 were the same as previously published research (Yao et al., 2012), indicating that the two MBs were suitable for our ensuring experiments. We found that miR-155 MBs could combine with the miR-155 gene and generate green fluorescent signals in CD133+/CD338+ cells (Figure 4A), as detected in the cell membrane of living CD133+/CD338+cells. Hochest 33342 staining was also detected in the cell membrane of living CD133+/CD338+ cells for a dye efflux capacity. Moreover, the control MB did not generate a green fluorescent signal in the CD133+/CD338+ cells (Figure 4A):the relative fluorescence intensity was markedly increased in the presence of miR-155 MB compared to in the presence of RS MB (Figure 4B). Overall, miR-155 gene expression in the CD133+/CD338+ cells was higher than that in the A549 cells (Figure 4C).

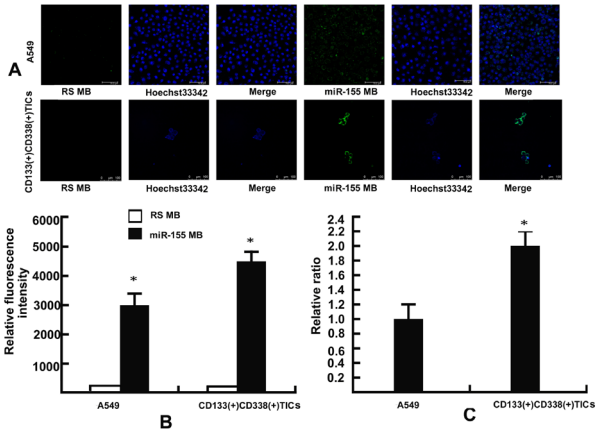

Figure 4. Intracellular Testing of miR-155 Expression using Confocal Microscopy. (A) A549 cells and CD133+/CD338+ cells were hybridized with RS MB or miR-155 MB. All cells were incubated with Hoechst 33342 (blue) (original magnification 40×). (B) The relative fluorescence intensity of the A549 cells and CD133+/CD338+ cells was detected (B). Scale bar, 75 mm. *$p < 0.05$, vs in the absence of the miR-155 sequence or the random sequence. (C) Real-time reverse-transcriptase polymerase chain reaction analysis of miR-155 in A549 and CD133+/CD338+ cells

Discussion

Despite the variety of drastic strategies, such as chemotherapy and radiotherapy, for the treatment of lung cancer, the prognosis of these patients remains poor. The identification and characterization of the tumorigenic cell population responsible for lung cancer formation and metastasis may contribute to the development of more effective diagnoses and therapies aiming at improving the prognosis of lung cancer (Eramo et al., 2008). In this study, we isolated and identified the population of CD133+/CD338+ cells as the lung cancer tumorigenic cell population. We found that CD133+/CD338+ cells sorted by MACS showed a greater potential for proliferation and increased tumorigenicity in vivo compared to A549 cells. We were able to detect miR-155 using molecular beacon technique and found that the expression of miR-155 was higher in CD133+/CD338+ cells than in A549 cells. Thus, miR-155 might serve as a biomarker in the diagnosis of lung cancer.

Recent studies have found that TICs exhibit some of the same specific surface molecular markers as some tumors. The cell surface marker CD133, a member of the cell membrane protein superfamily, was used to identify TICs as a specific marker in such solid tumors as a brain tumor (Singh et al., 2003; Singh et al., 2004), hepatocellular carcinoma (Suetsugu et al., 2006; Yin et al., 2007), pancreatic cancer (Hermann et al., 2007), prostate cancer (Collins et al., 2005), colon cancer (O'Brien et al., 2007; Ricci-Vitiani et al., 2007), and lung cancer (Eramo et al., 2008). Purified CD133+ TICs from these

cancers showed the potential of self-renewal capacity, differentiation, and proliferation and had the capability to form tumors in immunodeficient mice (Collins et al., 2005; Suetsugu et al., 2006; O'Brien et al., 2007). The $CD133^+$ cells from fresh lung tumor samples were also found to have tumor-initiating properties in both small cell and non-small cell lung cancers (Eramo et al., 2008). However, some evidence has indicated that the ability of $CD133^+$ expression to discriminate lung TICs may have been overestimated (Sullivan et al., 2010) and that $CD133^+$ cells do not represent TICs (Meng et al., 2009). Thus, the CD133 marker should be combined with other cell surface markers for the isolation and identification of lung TICs. CD338 (ABCG2), a member of the ATP-binding cassette (ABC) transporter superfamily, is an important determinant of the side population (SP) phenotype (Zhou et al., 2001). SP cells expressing marked by CD338 have stem cell-like capabilities that have found in a variety of solid malignancies and NSCLC (Ho et al., 2007). Furthermore, CD338 can promote resistance to multiple drugs and has been observed in many types of TICs (Bertolini et al., 2009). Lung cancer stem cells, isolated with Hoechst 33342, were found to express significantly higher levels of CD338 (Seo et al., 2007). In our study, we found that the TICs we isolated strongly had highly expressed $CD133^+/CD338^+$, possessed proliferation and enhanced tumorigenesis capacities, and more highly expressed of stem cell-associated genes. These results demonstrate that $CD133^+/CD338^+$ cells might be TICs with tumor-initiating capacity in NSCLC.

Increasing evidence shows that miRNAs can regulate TICs, and aberrant miRNAs in TICs may help in the understanding the mechanism of tumorigenesis, therapy-resistance, recurrence, and metastasis (Yu et al., 2010; Wu et al., 2012; Yu et al., 2012; Kwon and Shin, 2013). miR-155 plays an important role in various physiological and pathological processes (Faraoni et al., 2009; Elton et al., 2012) and has been found to be upregulated in several solid tumors, such as clear-cell kidney cancer (Juan et al., 2010), hepatocellular carcinoma (Wang et al., 2009a), breast cancer (Jiang et al., 2010; Kong et al., 2010), pancreatic cancer (Habbe et al., 2009; Greither et al., 2010; Ryu et al., 2010), and lung cancer (Yanaihara et al., 2006; Donnem et al., 2011). Moreover, high miR-155 expression is associated with a poor prognosis in lung cancer (Yanaihara et al., 2006; Donnem et al., 2011), suggesting that elevated miR-155 expression might be a prognostic biomarker of lung cancer (Xie et al., 2010).

Molecular beacons are single-stranded oligonucleotide hybridization probes that form a stem-and-loop structure. In the absence of a complementary miRNA target, molecular beacons form a stem-loop structure and do not fluoresce. However when they hybridize to their complementary miRNA sequence, these beacons undergo a conformational change that enables them to fluoresce upon excitation (Santangelo et al., 2006). Due to their stem structure, the recognition of targets by molecular beacons is so specific that if the target differs even by a single nucleotide, the probe does not bind to it. Furthermore, molecular beacons can be modified with locked nucleic acids (LNAs) to ensure a greater stability of the probe and enable the simultaneous detection of multiple targets (Tyagi and Kramer, 1996; Tyagi et al., 1998) .

In summary, we successfully isolated and identified a cellular subpopulation expressing $CD133^+/CD338^+$ that could represent TICs of the A549 cell line, and miR-155 was efficiently and specifically detected by a miR-155 MB in TICs. Molecular beacons have the potential to serve as powerful tools for quantifying miRNA expression in biological specimens. We believe that molecular beacons could be used to detect miRNAs in various tissues during carcinogenesis.

Acknowledgements

This work was supported by the National Natural Science Foundation of China (No. 81071786 and No. 81172070) and the National High Technology Research and Development Program of China (No. 2008AA02Z104).

References

Adhikari AS, Agarwal N, Iwakuma T (2011). Metastatic potential of tumor-initiating cells in solid tumors. *Front Biosci*, **16**, 1927-38.

Bartel DP (2004). MicroRNAs: genomics, biogenesis, mechanism, and function. *Cell*, **116**, 281-97.

Bertolini G, Roz L, Perego P, et al (2009). Highly tumorigenic lung cancer $CD133^+$ cells display stem-like features and are spared by cisplatin treatment. *Proc Natl Acad Sci USA*, **106**, 16281-6.

Bushati N, Cohen SM (2007). microRNA functions. *Annu Rev Cell Dev Biol*, **23**, 175-205.

Chen CZ (2005). MicroRNAs as oncogenes and tumor suppressors. *N Engl J Med*, **353**, 1768-71.

Collins AT, Berry PA, Hyde C, Stower MJ, Maitland NJ (2005). Prospective identification of tumorigenic prostate cancer stem cells. *Cancer Res*, **65**, 10946-51.

Donnem T, Eklo K, Berg T, et al (2011). Prognostic impact of MiR-155 in non-small cell lung cancer evaluated by in situ hybridization. *J Transl Med*, **9**, 6.

Elton TS, Selemon H, Elton SM, Parinandi NL (2012). Regulation of the MIR155 host gene in physiological and pathological processes. *Gene*, **532**, 1-12

Eramo A, Lotti F, Sette G, et al (2008). Identification and expansion of the tumorigenic lung cancer stem cell population. *Cell Death Differ*, **15**, 504-14.

Faraoni I, Antonetti FR, Cardone J, Bonmassar E (2009). miR-155 gene: a typical multifunctional microRNA. *Biochim Biophys Acta*, **1792**, 497-505.

Garofalo M, Croce CM (2011). microRNAs: Master regulators as potential therapeutics in cancer. *Annu Rev Pharmacol Toxicol*, **51**, 25-43.

Garzon R, Calin GA, Croce CM (2009). MicroRNAs in Cancer. *Annu Rev Med*, **60**, 167-79.

Georgantas RW, Hildreth R, Morisot S, et al (2007). CD34+ hematopoietic stem-progenitor cell microRNA expression and function: a circuit diagram of differentiation control. *Proc Natl Acad Sci USA*, **104**, 2750-5.

Greither T, Grochola LF, Udelnow A, et al (2010). Elevated expression of microRNAs 155, 203, 210 and 222 in pancreatic tumors is associated with poorer survival. *Int J Cancer*, **126**, 73-80.

Guo W, Lasky JL, Wu H (2006). Cancer stem cells. *Pediatr Res*, **59**, 59-64.

Habbe N, Koorstra JB, Mendell JT, et al (2009). MicroRNA miR-155 is a biomarker of early pancreatic neoplasia. *Cancer Biol Ther*, **8**, 340-6.

Hatfield S, Ruohola-Baker H (2008). microRNA and stem cell function. *Cell Tissue Res*, **331**, 57-66.

Henschke CI, Yankelevitz DF, Libby DM, et al (2006). Survival of patients with stage I lung cancer detected on CT screening. *N Engl J Med*, **355**, 1763-71.

Hermann PC, Huber SL, Herrler T, et al (2007). Distinct populations of cancer stem cells determine tumor growth and metastatic activity in human pancreatic cancer. *Cell Stem Cell*, **1**, 313-23.

Ho MM, Ng AV, Lam S, Hung JY (2007). Side population in human lung cancer cell lines and tumors is enriched with stem-like cancer cells. *Cancer Res*, **67**, 4827-33.

Jemal A, Siegel R, Ward E, et al (2006). Cancer statistics, 2006. *CA Cancer J Clin*, **56**, 106-30.

Jiang S, Zhang HW, Lu MH, et al (2010). MicroRNA-155 functions as an OncomiR in breast cancer by targeting the suppressor of cytokine signaling 1 gene. *Cancer Res*, 70, 3119-27.

Juan D, Alexe G, Antes T, et al (2010). Identification of a microRNA panel for clear-cell kidney cancer. *Urology*, **75**, 835-41.

Kim Y, Yang CJ, Tan W (2007). Superior structure stability and selectivity of hairpin nucleic acid probes with an L-DNA stem. *Nucleic Acids Res*, **35**, 7279-87.

Kong W, He L, Coppola M, et al (2010). MicroRNA-155 regulates cell survival, growth, and chemosensitivity by targeting FOXO3a in breast cancer. *J Biol Chem*, **285**, 17869-79.

Krol J, Loedige I, Filipowicz W (2010). The widespread regulation of microRNA biogenesis, function and decay. *Nat Rev Genet*, **11**, 597-610.

Kwak PB, Iwasaki S, Tomari Y (2010). The microRNA pathway and cancer. *Cancer Sci*, **101**, 2309-15.

Kwon MJ, Shin YK (2013). Regulation of ovarian cancer stem cells or tumor-initiating cells. *Int J Mol Sci*, **14**, 6624-48.

Meng X, Li M, Wang X, Wang Y, Ma D (2009). Both $CD133^+$ and CD133- subpopulations of A549 and H446 cells contain cancer-initiating cells. *Cancer Sci*, **100**, 1040-6.

O'Brien CA, Pollett A, Gallinger S, Dick JE (2007). A human colon cancer cell capable of initiating tumour growth in immunodeficient mice. *Nature*, **445**, 106-10.

Ricci-Vitiani L, Lombardi DG, Pilozzi E, et al (2007). Identification and expansion of human colon-cancer-initiating cells. *Nature*, **445**, 111-5.

Ryu JK, Hong SM, Karikari CA, et al (2010). Aberrant MicroRNA-155 expression is an early event in the multistep progression of pancreatic adenocarcinoma. *Pancreatology*, **10**, 66-73.

Santangelo P, Nitin N, Bao G (2006). Nanostructured probes for RNA detection in living cells. *Ann Biomed Eng*, **34**, 39-50.

Seo DC, Sung JM, Cho HJ, et al (2007). Gene expression profiling of cancer stem cell in human lung adenocarcinoma A549 cells. *Mol Cancer*, **6**, 75.

Singh SK, Clarke ID, Terasaki M, et al (2003). Identification of a cancer stem cell in human brain tumors. *Cancer Res*, **63**, 5821-8.

Singh SK, Hawkins C, Clarke ID, et al (2004). Identification of human brain tumour initiating cells. Nature, **432**, 396-401.

Suetsugu A, Nagaki M, Aoki H, et al (2006). Characterization of $CD133^+$ hepatocellular carcinoma cells as cancer stem/progenitor cells. *Biochem Biophys Res Commun*, **351**, 820-824.

Sullivan JP, Minna JD, Shay JW (2010). Evidence for self-renewing lung cancer stem cells and their implications in tumor initiation, progression, and targeted therapy. *Cancer Metastasis Rev*, **29**, 61-72.

Tyagi S, Bratu DP, Kramer FR (1998). Multicolor molecular beacons for allele discrimination. *Nat Biotechnol*, **16**, 49-53.

Tyagi S, Kramer FR (1996). Molecular beacons: probes that fluoresce upon hybridization. *Nat Biotechnol*, **14**, 303-8.

Wang B, Majumder S, Nuovo G, et al (2009a). Role of microRNA-155 at early stages of hepatocarcinogenesis induced by choline-deficient and amino acid-defined diet in C57BL/6 mice. *Hepatology*, **50**, 1152-61.

Wang QZ, Xu W, Habib N, Xu R (2009b). Potential uses of microRNA in lung cancer diagnosis, prognosis, and therapy. *Curr Cancer Drug Targets*, **9**, 572-94.

Wu K, Ding J, Chen C, et al (2012). Hepatic transforming growth factor beta gives rise to tumor-initiating cells and promotes liver cancer development. *Hepatology*, **56**, 2255-67.

Xie Y, Todd NW, Liu Z, et al (2010). Altered miRNA expression in sputum for diagnosis of non-small cell lung cancer. *Lung Cancer,* **67**, 170-6.

Yanaihara N, Caplen N, Bowman E, et al (2006). Unique microRNA molecular profiles in lung cancer diagnosis and prognosis. *Cancer Cell*, **9**, 189-98.

Yao Q, Zhang AM, Ma H, et al (2012). Novel molecular beacons to monitor microRNAs in non-small-cell lung cancer. *Mol Cell Probes*, **26**, 182-7.

Yin S, Li J, Hu C, et al (2007). CD133 positive hepatocellular carcinoma cells possess high capacity for tumorigenicity. *Int J Cancer,* **120**, 1444-50.

Yu F, Deng H, Yao H, et al (2010). Mir-30 reduction maintains self-renewal and inhibits apoptosis in breast tumor-initiating cells. *Oncogene*, **29**, 4194-204.

Yu F, Jiao Y, Zhu Y, et al (2012). MicroRNA 34c gene down-regulation via DNA methylation promotes self-renewal and epithelial-mesenchymal transition in breast tumor-initiating cells. *J Biol Chem*, **287**, 465-73.

Zandberga E, Kozirovskis V, Abols A, et al (2013). Cell-free microRNAs as diagnostic, prognostic, and predictive biomarkers for lung cancer. *Genes Chromosomes Cancer*, **52**, 356-69.

Zhou S, Schuetz JD, Bunting KD, et al (2001). The ABC transporter Bcrp1/ABCG2 is expressed in a wide variety of stem cells and is a molecular determinant of the side-population phenotype. *Nat Med*, **7**, 1028-34.